Vol. 527: 59–71, 2015
doi: 10.3354/meps11218

MARINE ECOLOGY PROGRESS SERIES
Mar Ecol Prog Ser

Published May 7

Responses of autotrophic and heterotrophic rates of plankton from a subtropical coastal site to short-term temperature modulations

Bingzhang Chen*, Kailin Liu

State Key Laboratory of Marine Environmental Science and Fujian Provincial Joint Key Laboratory of Coastal Ecology and Environmental Studies, Xiamen University, Xiamen, Fujian, PR China

ABSTRACT: We investigated the responses of plankton collected throughout a seasonal cycle from a eutrophic, subtropical coastal site near Xiamen, China to short-term temperature modulations from the *in situ* ambient temperature. We used linear mixed effect models to estimate the temperature coefficients (i.e. activation energy) and tested the hypothesis that the activation energies of autotrophic rates (i.e. phytoplankton growth and photosynthesis) are lower than those of heterotrophic rates (i.e. microzooplankton grazing and community respiration). However, we found that there were no significant differences of activation energy (~0.65 eV) between autotrophic and heterotrophic rates. Based on both physiological and statistical grounds, we argue that the inherent activation energies of phytoplankton photosynthesis and growth rates may not be lower than 0.65 eV in some instances.

KEY WORDS: Temperature · Phytoplankton · Growth · Grazing · Activation energy · Photosynthesis · Respiration

INTRODUCTION

Temperature is an important factor that affects ecosystem properties such as primary production, community structure, trophic interactions, food web stability, and carbon export (Laws et al. 2000, Sarmiento et al. 2004, Taucher & Oschlies 2011). It is vital to reliably quantify the temperature sensitivity of these key ecological fluxes to evaluate the effects of global warming to our ecosystem (Vasseur & McCann 2005, Fussmann et al. 2014). The temperature sensitivity of photosynthesis has been claimed to be lower than that of heterotrophic processes such as respiration and grazing rates (López-Urrutia et al. 2006, Rose & Caron 2007, Regaudie-De-Gioux & Duarte 2012). If we use the Arrhenius equation to describe the temperature dependence of metabolic rates, the activation energy of photosynthesis or phytoplankton growth rate is often estimated between 0.3 and 0.4 eV, approximately equivalent to Q_{10} factors of ~1.5 to 1.8 (Eppley 1972, López-Urrutia et al. 2006, Rose & Caron 2007, Bissinger et al. 2008, Sal & López-Urrutia 2011, Chen et al. 2012, Regaudie-De-Gioux & Duarte 2012). Note that the activation energy can be transformed to the conventional Q_{10} factor following the formula:

$$Q_{10} = e^{\frac{10E\left(\frac{1}{T_c} - \frac{1}{T}\right)}{k\left(T - T_c\right)}}$$

where E is the activation energy, T is the absolute temperature (K), T_c is a reference temperature (288.15 K in this study), and k is the Boltzmann's constant (8.62×10^{-5} eV K^{-1}). By contrast, the activation energies of heterotrophic rates such as zooplankton growth and grazing and community respiration are estimated between 0.6 and 0.7 eV ($Q_{10} \approx 2.2$ to 2.8) (Rose & Caron 2007, Chen et al. 2012, Regaudie-De-

*Corresponding author: bzchen2011@xmu.edu.cn

Gioux & Duarte 2012), values consistent with the metabolic theory of ecology (Brown et al. 2004). The implication is that increasing temperature could force the ecosystem to become more heterotrophic, whereby respiration exceeds photosynthesis. Other things being equal, this would result in more CO_2 being released into the atmosphere (López-Urrutia et al. 2006). In a closed system, in which photosynthesis ultimately determines respiration, the greater temperature sensitivity of respiration implies a reduction of heterotrophic biomass compared to autotrophic biomass (Allen et al. 2005, Yvon-Durocher et al. 2012). The lower sensitivity of phytoplankton growth rates to temperature compared to those of zooplankton is also attributed to the occurrences of phytoplankton blooms at high latitudes (Rose & Caron 2007).

Most reported estimates of *E* of plankton rates are based on a single regression on pooled datasets (of rate vs. temperature) that combine the rates of the same taxa/assemblages measured at different temperatures with those of different taxa/assemblages at different temperatures (Tang 1995, López-Urrutia et al. 2006, Chen et al. 2012). These estimates might differ from those based on a single taxon or assemblage. At an ecosystem level, changes in community composition may affect estimations of temperature sensitivity (Yvon-Durocher et al. 2012). Species living in cold environments might have evolved to adapt to the cold so that the activation energy estimated among species could be lower than within species (Clarke & Johnston 1999, Clarke 2004, Gaston et al. 2009). Estimating temperature sensitivity across taxa may be more suitable for large-scale studies in which changes of community composition are ubiquitous. Conversely, estimates of temperature sensitivity for the same taxa/assemblages should be more appropriate for local scales. Significant heterogeneity exists among activation energies, which may vary with functional groups and different ecological processes (Dell et al. 2011, Huey & Kingsolver 2011, Fussmann et al. 2014).

Statistical issues emerge when estimating temperature sensitivity from a pooled dataset. Some critical assumptions such as independence of errors are not always rigorously checked in studies that use linear regressions to estimate activation energy (Faraway 2004). Such datasets are usually hierarchical, that is, repeated data pairs of growth rate and temperature exist for a same taxon or assemblage and different taxa and assemblages appear at different temperatures. This kind of data structure introduces an 'intraclass correlation' and mixed-effect models should be used (Zuur et al. 2009).

In this study, we quantify the temperature sensitivities of phytoplankton growth and microzooplankton grazing rates as well as photosynthesis and respiration rates to short-term experimental temperature modulations along a seasonal cycle in a subtropical eutrophic environment. Our results suggest that the difference of activation energy between autotrophic and heterotrophic rates might be not as significant as has been thought.

MATERIALS AND METHODS

Plankton were collected at a coastal site (24° 20′ 42″ N, 118° 11′ 8″ E) near Xiamen, Fujian Province, China (Fig. 1) between December 2012 and March 2014. We measured the responses of phytoplankton growth and microzooplankton grazing rates to short-term temperature modulations from the *in situ* ambient temperature using the dilution technique. We also measured gross primary production (*GPP*) and community respiration (*CR*) rates using light-dark bottle incubations under the same environmental settings.

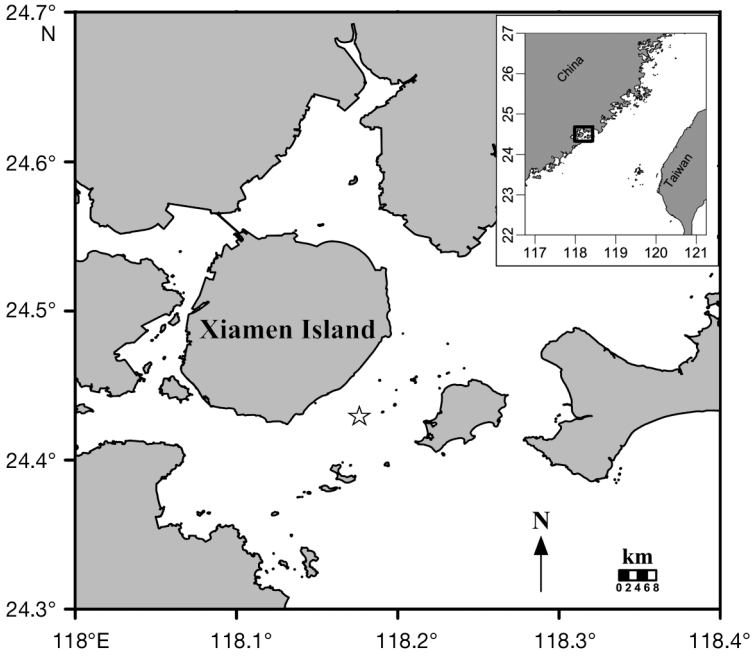

Fig. 1. Location of sampling station (☆) where plankton were collected at a subtropical coastal site near Xiamen, Fujian Province, China

We set up a gradient of 4 or 5 temperatures for each experiment (T_s – 4°C, T_s – 2°C, T_s, T_s + 3°C, and T_s + 5°C, where T_s = *in situ* ambient temperature) and conducted 'mini-dilution' experiments at each temperature (Landry et al. 1984, 2008, Worden & Binder 2003, Strom & Fredrickson 2008). We set up 2 dilution levels (15% and 100%) with duplicate bottles for each level. We prepared particle-free water by gravity filtering the seawater through a 0.2 µm filter capsule (Pall Corporation) and then added measured volumes of filtered seawater into 1 l polycarbonate bottles to attain the desired dilution levels. The bottles were then gently filled with unfiltered seawater to full capacity. Two additional bottles filled with unfiltered seawater were sacrificed for initial samples of chlorophyll *a* (chl *a*), and for flow cytometric (FCM) and microscopic analyses. To ensure that phytoplankton growth rates were not limited by inorganic nutrients, we added nutrients (final concentrations: 0.8 µmol l^{-1} nitrate and 0.05 µmol l^{-1} phosphate) into the bottles. We also set up control bottles without nutrient enrichment at the *in situ* temperature to assess the nutrient effects.

All bottles were tightly capped and incubated for 24 h in an incubator with 5 temperature gradients (FIRSTEK) with the light intensity of 130 µmol photons cm^{-2} h^{-1}. After incubation, samples were taken from each bottle for chl *a*, pigment and FCM analyses. All tubings and bottles were thoroughly acid-washed and rinsed with MilliQ water before each experiment.

For chl *a* analyses, 100 ml of seawater was filtered onto 25 mm glass-fibre GF/F filters (Whatman) under low vacuum (<150 mm Hg). After being frozen at –80°C for 1 d, the filters were soaked in 90% acetone for 20 h and the fluorescence was measured using the non-acidification method on a Turner Designs fluorometer (Welschmeyer 1994).

FCM samples were fixed with 0.5% buffered paraformadehyde and frozen at –80°C until analysis (Vaulot et al. 1989). Two populations of picophytoplankton (i.e. *Synechococcus*, and picoeukaryotes) were delineated and enumerated based on light scattering and fluorescence on a Becton-Dickson FACSCalibur flow cytometer (Olson et al. 1993). The exact flow rate was calibrated by weighing a tube filled with distilled water before and after running for certain time intervals and the flow rate was estimated as the slope of a linear regression between elapsed time and weight reductions (Li & Dickie 2001).

Accessory pigment concentrations were measured by high performance liquid chromatography (HPLC) according to Furuya et al. (1998). One liter of seawater was filtered onto glass-fiber GF/F filters under low vacuum (<150 mm Hg). The filters were frozen at –80°C for 1 to 6 mo until analysis. Upon return to the laboratory, the filters were soaked in 2 ml N,N-dimethylformamide (DMF) at –20 °C for 1 h. The extractions were then filtered through 13 mm GF/F filters to clean the debris and mixed with ammonium acetate solution (1 mol l^{-1}) at 1:1 ratio. Each mixture was partially injected into an DIONEX UltiMate 3000 HPLC system fitted with a 3.5 µm Eclipse XDB C_8 column (100 × 4.6 mm; Agilent Technologies). Quantification was confirmed by the standards purchased from the Danish Hydraulic Institute Water and Environment.

We quantified the contribution of each phytoplankton group to total chl *a* concentration using the program CHEMTAX implemented under the MATLAB platform (MathWorks;Mackey et al. 1996). Combinations of 13 pigment markers were used to represent 7 phytoplankton classes, including dinoflagellates, diatoms, haptophytes, chlorophytes, cryptophytes, *Synechococcus* and prasinophytes. The ratios of initial inputting pigment:chl *a* ratio (F_{input}) followed previous studies (Mackey et al. 1996). Successive runs were implemented for convergence between input and output ratio (F_{output}) (Latasa 2007).

Samples (100 ml) for enumeration of microzooplankton (including ciliates, dinoflagellates, and copepod nauplii) were fixed with 5% acidic Lugol's solution (final concentration) and stored in the dark at room temperature. After sedimentation for 24 h, the microplankton cells were counted under an Olympus IX51 inverted microscope using the Utermöhl method at 200× magnification. Biovolumes of ciliates, dinoflagellates and nauplii were also calculated using appropriate geometric formulae. The biovolume of ciliates was converted to cell carbon using the conversion factor of 0.19 pg C $µm^{-3}$ (Putt & Stoecker 1989). The biovolume ($µm^3$) of dinoflagellates was converted to cell carbon using the equation pg C $cell^{-1}$ = 0.76 × $volume^{0.819}$, according to Menden-Deuer & Lessard (2000). Carbon contents of nauplii were estimated from length (µm) using the equation pg C $cell^{-1}$ = 1.51 × 0.01 × $length^{2.94}$ (Uye 1996).

The growth rates of phytoplankton and microzooplankton grazing rates were estimated as follows. Assuming an exponential growth model, we calculated the net growth rate (k_i) of phytoplankton in each dilution treatment according to the formula $k_i = \ln[C_i/(D_i \times C_0)]$, where C_i was the phytoplankton concentration in the ith treatment bottle after incubation, D_i was the dilution level (15% or 100%) of the ith

treatment, and C_0 was the initial phytoplankton concentration. Phytoplankton growth and microzooplankton grazing rates were estimated following Landry et al. (2008). In cases where nutrients were added into the bottles, both nutrient-enriched growth rate (μ_n) and non-enriched growth rates (μ_c) were obtained. We used the synthesis and destruction rate of pigment markers to estimate the growth and grazing rates of corresponding phytoplankton groups to avoid the uncertainties in the CHEMTAX computation. Nutrient concentrations were measured following the standard protocol (Parsons et al. 1984).

GPP was estimated by measuring the changes of oxygen concentrations in 65 ml biological oxygen demand (BOD) bottles incubated under light and dark conditions. The exact volumes of the BOD bottles were calibrated prior to use. We gently siphoned the seawater into the glass-stoppered BOD bottles. The dark bottles were covered with aluminum foils. All the bottles were incubated under the same conditions as the dilution experiments. For each temperature, we set up quadruplicate bottles for initial, light, and dark bottles, respectively. The oxygen concentrations were titrated following the Winkler method using an automatic titration system (Metrohm 848) (Oudot et al. 1988). The coefficient variations of titrated oxygen concentrations were usually <0.5%.

To remove the inhibitory effect of artificially induced supraoptimal temperatures on the rate estimates, we removed the rates above the optimal growth temperatures before fitting the Arrhenius model. At least 3 effective data points were required for one experiment to be included in the mixed-effect modeling. We discarded zero and negative growth and grazing rates before model fitting. By this approach, 18, 28, 43, and 32% of the total data were removed, respectively, for phytoplankton growth, microzooplankton grazing, *GPP*, and *CR*. Retaining these data in the regression will lead to lower estimates of activation energy.

We used linear mixed effect models to allow random variations of both slopes and intercepts of the linear regression curves for each experiment:

$$\ln r_i = \left(\ln r_0 + \varepsilon_{r,i}\right) + \frac{\left(E_r + \varepsilon_{Er,i}\right)}{k}\left(\frac{1}{T_c} - \frac{1}{T}\right) \quad (1)$$

where r_i is the phytoplankton growth rate at temperature T (K) in the ith experiment; r_0 is the growth rate normalization at the reference temperature T_c (288.15 K); E_r is the mean activation energy for phytoplankton growth rate; $\varepsilon_{r,i}$ and $\varepsilon_{Er,i}$ are random deviations from ln r_0 and E_r, respectively; and k is the Boltzmann's constant (8.62×10^{-5} eV K^{-1}). Light and nutrient concentrations were not included in the model because light levels were kept constant in all experiments and nutrients were added during incubation.

As microzooplankton biomass is another important factor determining microzooplankton grazing rate (Landry et al. 2008, Chen et al. 2012), we included microzooplankton biomass (*MZ*, µg C l^{-1}) in the linear mixed-effect model to estimate the activation energy of microzooplankton grazing rate:

$$\ln m_i = \left(\ln m_0 + \varepsilon_{m,i}\right) + \alpha_1 lnMZ_i + \frac{\left(E_m + \varepsilon_{Em,i}\right)}{k}\left(\frac{1}{T_c} - \frac{1}{T}\right) \quad (2)$$

where m_i is the grazing rate at temperature T of the ith experiment; m_0 is the growth rate normalization at T_c; E_m is the mean activation energy of microzooplankton grazing rate; $\varepsilon_{m,i}$ and $\varepsilon_{Em,i}$ are random deviations from ln m_0 and E_m, respectively; and α_1 is an exponent constant describing the relationship between m and MZ.

For estimating the activation energy of *GPP* and *CR*, we included chl *a* concentration in the models (Regaudie-De-Gioux & Duarte 2012):

$$\ln GPP_i = \left(\ln GPP_0 + \varepsilon_{GPP,i}\right) + \alpha_2 lnChl_i + \frac{\left(E_{GPP} + \varepsilon_{EGPP,i}\right)}{k}\left(\frac{1}{T_c} - \frac{1}{T}\right) \quad (3)$$

$$\ln CR_i = \left(\ln CR_0 + \varepsilon_{CR,i}\right) + \alpha_3 lnChl_i + \frac{\left(E_{CR} + \varepsilon_{ECR,i}\right)}{k}\left(\frac{1}{T_c} - \frac{1}{T}\right) \quad (4)$$

with the notations similar to Eqs. (1) and (2). All the analyses were implemented with the package 'lme4' in the software R 3.1.1 (Bates et al. 2014, R Core Team 2014).

RESULTS

General conditions of the coastal site near Xiamen

In total, we performed 20 temperature-gradient dilution experiments. The *in situ* sea surface temperatures varied from 13°C in winter to 30°C in summer. Nitrate and phosphate concentrations were usually replete, with nitrate concentrations >15 µmol l^{-1} and

phosphate concentrations no less than 0.4 µmol l^{-1}. The phytoplankton community was dominated by diatoms, cryptophytes, and prasinophytes, which in total accounted for nearly 98 % of the total pigment biomass all year round (Fig. 2). There were no obvious changes of phytoplankton composition throughout the seasonal cycle. Chl *a* concentrations measured by the fluorometer were, on average, 1.5 times higher than those measured by HPLC and the 2 datasets showed consistent trends. Chl *a* concentrations measured by the fluorometer ranged from 0.42 to 15.4 µg l^{-1} and were positively correlated with temperature (Spearman correlation $r = 0.64$, $p < 0.001$). Dominated by ciliates and heterotrophic dinoflagellates, microzooplankton biomass ranged from 2.12 to 48.5 µg C l^{-1} and was highly positively correlated with chl *a* concentration (Spearman $r = 0.88$, $p < 10^{-5}$) and temperature (Spearman $r = 0.62$, $p < 0.01$) (Fig. 3).

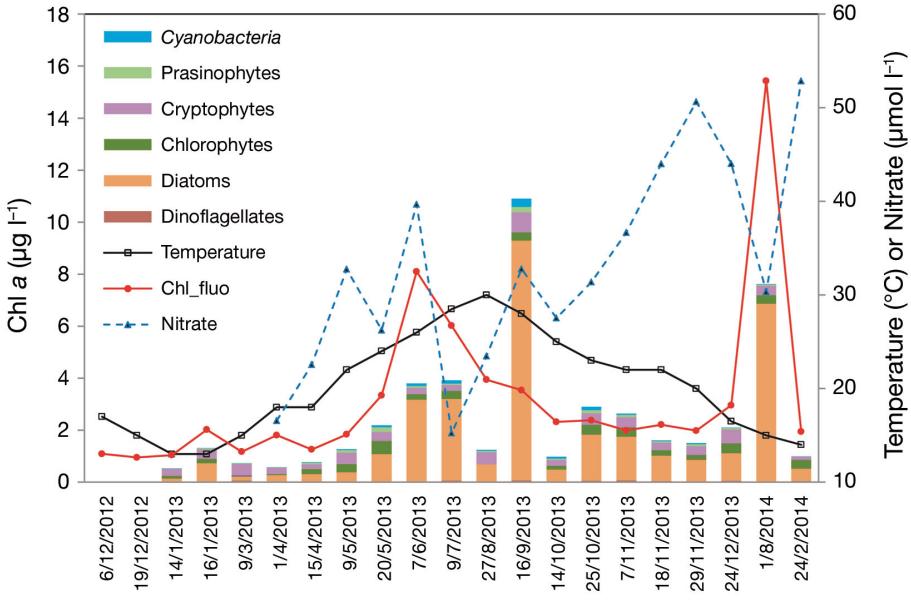

Fig. 2. Seasonal variation of temperature, nitrate, and chl *a* concentrations measured by fluorometry (Chl_fluo) (lines). Colored bars indicate chl *a* concentrations by subgroup measured by HPLC. Note the difference of chl *a* concentrations between the fluorometry and the HPLC method. Dinoflagellates were found in all samples at trace amounts (<2 %). Sampling dates given as d/mo/yr

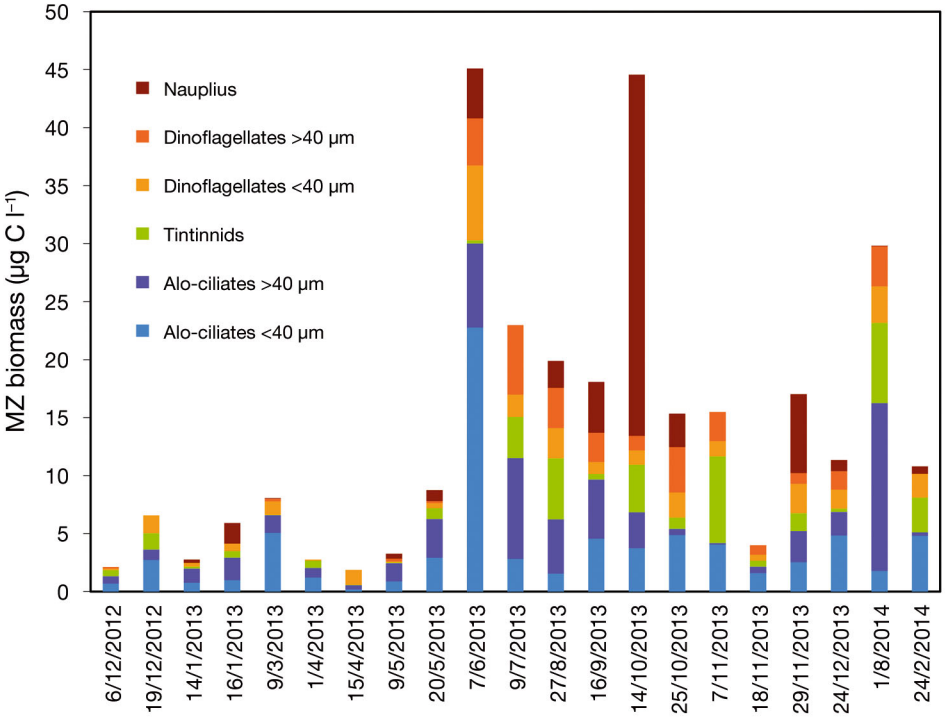

Fig. 3. Biomass of microzooplankton (MZ) groups of the dilution experiments, with dinoflagellates and aloricate (Alo) ciliates subdivided by equivalent spherical diameter (>40 µm and <40 µm). Sampling dates given as d/mo/yr

Temperature sensitivity of bulk phytoplankton growth rate and microzooplankton grazing rate

After we removed the phytoplankton growth rates at supraoptimal temperatures, the mean activation energy of the growth rate of bulk phytoplankton assemblages estimated by the linear mixed-effect model was 0.71 ± 0.08 eV (mean ± SE; Fig. 4), close to the 0.65 eV predicted by the classic metabolic theory of ecology (Brown et al. 2004). Consistent with the high ambient nutrient concentrations, the nutrient additions significantly increased phytoplankton growth rates in only 1 experiment ($p < 0.05$), close to the probability of Type-I error. There were significant random variations associated with the activation energies ($\chi^2 = 8.2$, $p < 0.05$; Table 1). The linear mixed-effect model including both fixed and random effects explained 85% of the total variance of phytoplankton growth rate, while fixed effects alone only explained 60%. The mean activation energy of microzooplankton grazing rate was also insignificantly different from 0.65 eV or that of phytoplankton growth rate (Table 1, Fig. 5). As including the variable of microzooplankton biomass did not improve the model ($\chi^2 = 0.05$, $p > 0.05$) and microzooplankton biomass was highly correlated with temperature, we excluded the variable of microzooplankton biomass from the linear mixed-effect model. The linear mixed effect model also accounted for a substantial fraction of the total variance of the microzooplankton grazing rate (Table 1).

Table 1. Normalization constants (ln r_0) and estimated mean ± SE activation energies (E, eV) of autotrophic and heterotrophic rates of plankton from a eutrophic, subtropical coastal site near Xiamen, China. σ_r and σ_E: standard deviations of the random effects for ln r_0 and E, respectively; μ_n: phytoplankton growth rate (d^{-1}); m: microzooplankton grazing rate (d^{-1}); *GPP*: gross primary production (µmol O_2 l^{-1} d^{-1}); *CR*: community respiration (µmol O_2 l^{-1} d^{-1}); N_o: number of observations; N_e: number of experiments; R^2_{fr}: percentage of variance explained by both fixed and random effects; R^2_f: percentage of variance explained only by fixed effects

Rate	ln r_0	E	σ_r	σ_E	R^2_{fr}	R^2_f	N_e	N_o
μ_n	−0.28 ± 0.12	0.71 ± 0.08	0.45	0.22	0.85	0.60	20	81
m	−1.75 ± 0.30	1.01 ± 0.19	0.99	0.51	0.77	0.41	16	58
GPP	1.44 ± 0.29	0.76 ± 0.13	0.44		0.93	0.78	10	38
CR	1.38 ± 0.39	0.60 ± 0.15	1.30	0.35	0.93	0	12	45

Temperature sensitivity of *GPP* and *CR*

The mean activation energies of *GPP* and *CR* were also not significantly different from 0.65 eV (Table 1, Figs. 6 & 7). There was a significantly positive effect of chl *a* concentration on *GPP* ($\chi^2 = 23.7$, $p < 0.001$), but not on *CR*. The random variations associated with the activation energy were insignificant for *GPP* ($\chi^2 = 2.8$, $p > 0.05$), so the estimated activation energy was the same for each experiment (Fig. 6). However, the variations were significant for *CR* ($\chi^2 = 8.5$, $p < 0.05$; Fig. 7).

Temperature sensitivity of growth and microzooplankton grazing rate of phytoplankton subgroups

The activation energies of growth and grazing rates of most phytoplankton groups except *Synechococcus* (HPLC) and dinoflagellates (only for growth) were insignificantly different from 0.65 eV (Tables 2 & 3). Possibly due to the small number of observa-

Table 2. Normalization constants (ln r_0) and estimated mean ± SE activation energies (E, eV) of growth rates of phytoplankton subgroups in response to temperature modulations. See Table 1 legend for key to symbols and abbreviations. FCM: flow cytometry; HPLC: high-performance liquid chromatography. We used zeaxanthin, fucoxanthin, prasinoxanthin, alloxanthin, peridinin, and chl *b* to represent *Synechococcus* (HPLC), diatoms, prasinophytes, cryptophytes, dinoflagellates, and green algae, respectively

Phytolankton group	ln r_0	E	σ_r	σ_E	R^2_{fr}	R^2_f	N_e	N_o
Synechococcus (FCM)	−0.42 ± 0.18	0.71 ± 0.11	0.58		0.73	0.22	17	73
Synechococcus (HPLC)	0.09 ± 0.13	0.46 ± 0.08	0.36		0.77	0.20	11	48
Picoeukaryotes	0.04 ± 0.10	0.60 ± 0.10	0.34	0.37	0.95	0.60	18	75
Diatoms	0.05 ± 0.12	0.59 ± 0.07	0.35		0.79	0.39	12	52
Prasinophytes	0.11 ± 0.12	0.52 ± 0.07	0.35		0.80	0.40	12	53
Cryptophytes	−0.68 ± 0.24	0.54 ± 0.12	0.67		0.82	0.15	9	40
Dinoflagellates	−0.26 ± 0.21	0.38 ± 0.10	0.49		0.72	0	7	28
Green algae	−0.16 ± 0.13	0.61 ± 0.10	0.32		0.67	0.34	11	47

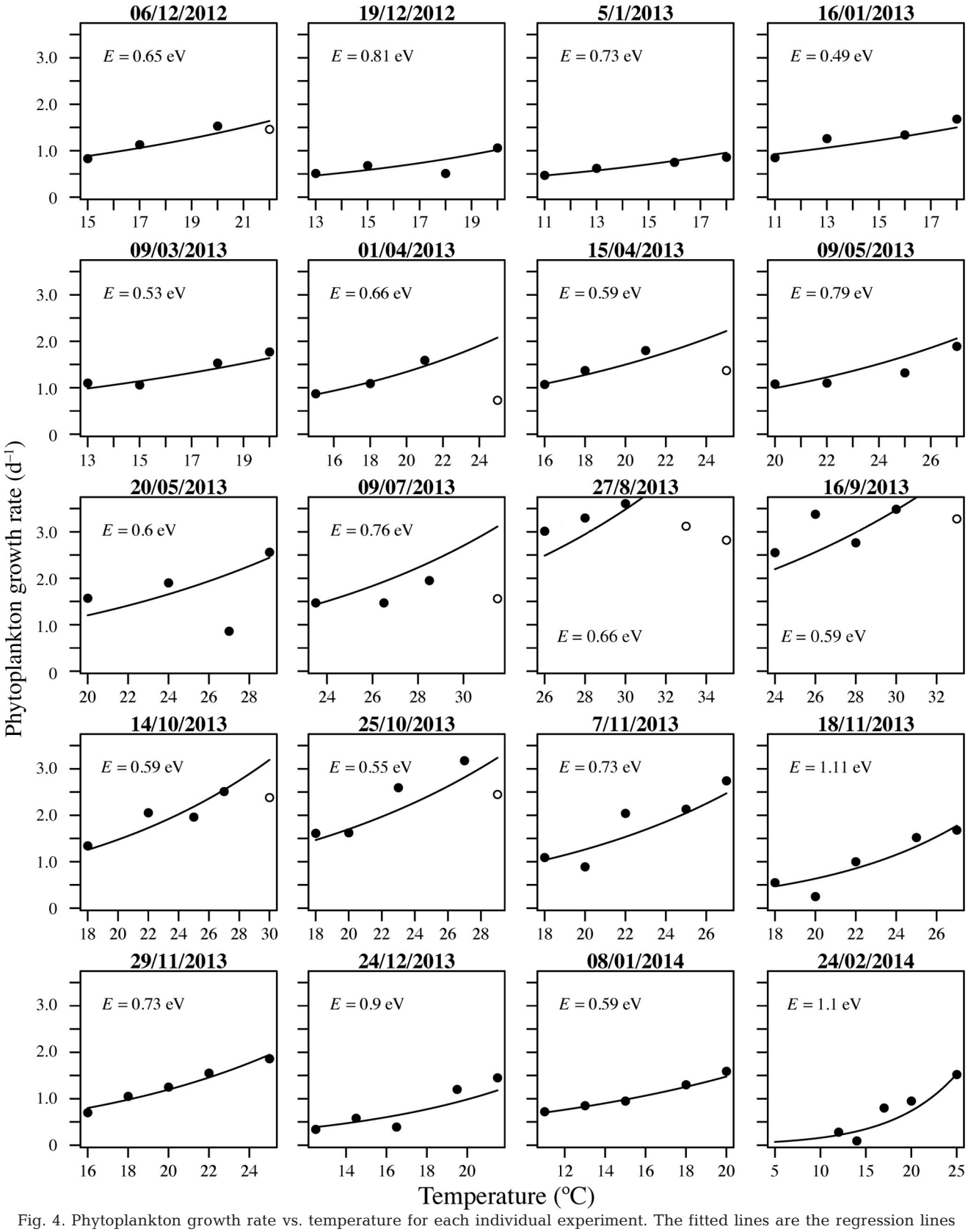

Fig. 4. Phytoplankton growth rate vs. temperature for each individual experiment. The fitted lines are the regression lines obtained from the linear mixed-effect model. *E*: activation energy. Open circles: data not used in fitting the linear mixed-effect models

Table 3. Normalization constants (ln r_0) and estimated mean ± SE activation energies (E, eV) and associated random effects of microzooplankton grazing rate (d^{-1}) on various phytoplankton groups. Symbols and abbreviations as in Tables 1 & 2

	ln r_0	E	σ_r	R^2_{fr}	R^2_f	N_e	N_o
Synechococcus (FCM)	−0.92 ± 0.17	0.53 ± 0.11	0.41	0.78	0.64	12	46
Synechococcus (HPLC)	−0.88 ± 0.24	0.41 ± 0.20	0.48	0.46	0.05	9	32
Picoeukaryotes	−0.94 ± 0.22	0.67 ± 0.17	0.50	0.79	0.40	10	35
Diatoms	−1.16 ± 0.25	0.69 ± 0.19	0.41	0.63	0.40	6	22
Prasinophytes	−1.75 ± 0.37	0.95 ± 0.29	0.49	0.68	0.39	6	20
Cryptophytes	−1.79 ± 0.19	0.88 ± 0.16	0.33	0.71	0.57	7	27
Dinoflagellates	−1.50 ± 0.32	0.73 ± 0.25	0.50	0.57	0.31	6	24
Green algae	−1.30 ± 0.42	1.05 ± 0.41	0.78	0.59	0.07	6	20

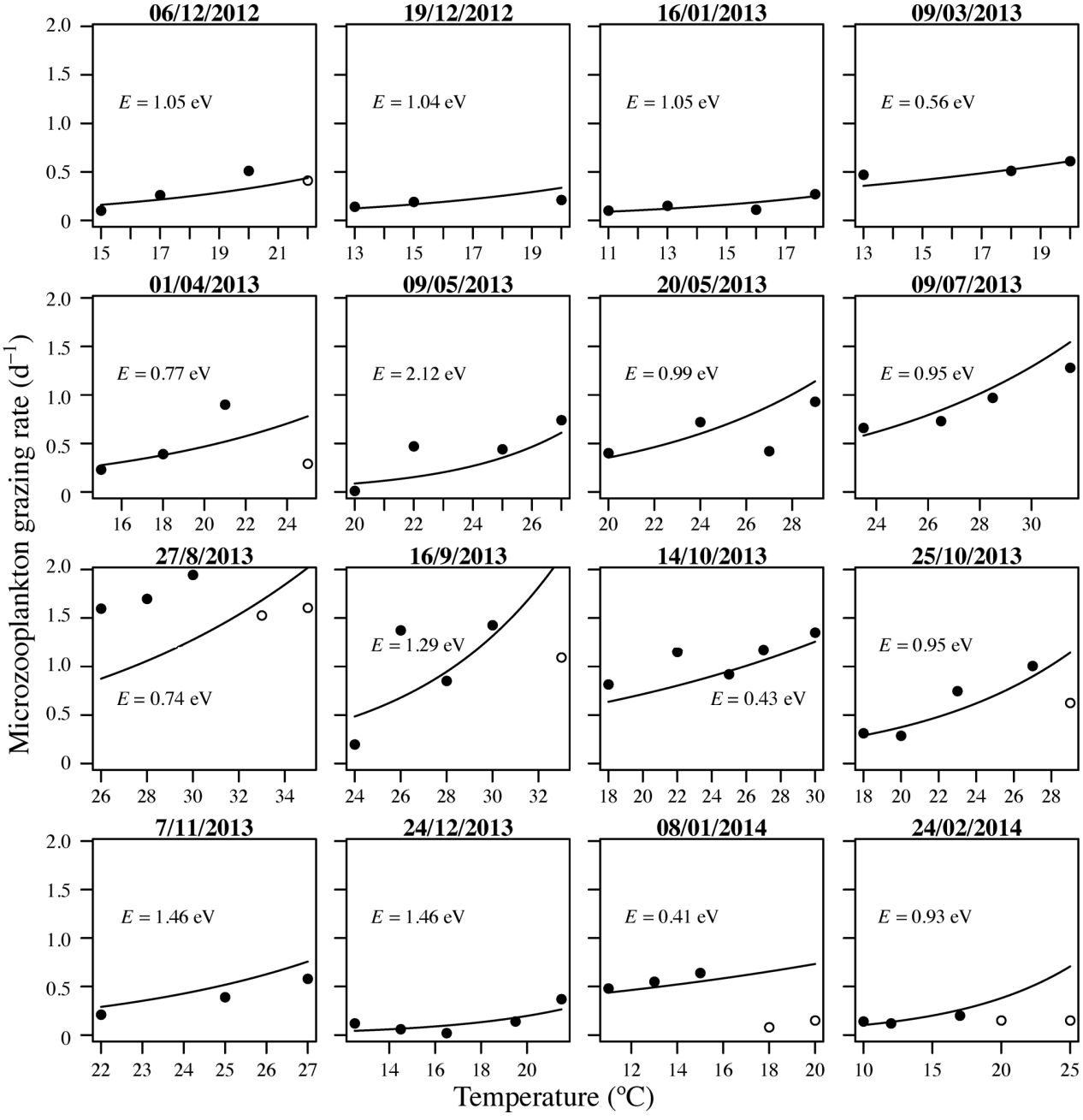

Fig. 5. Microzooplankton grazing rate vs. temperature for each individual experiment. Symbols and abbreviations as in Fig. 4

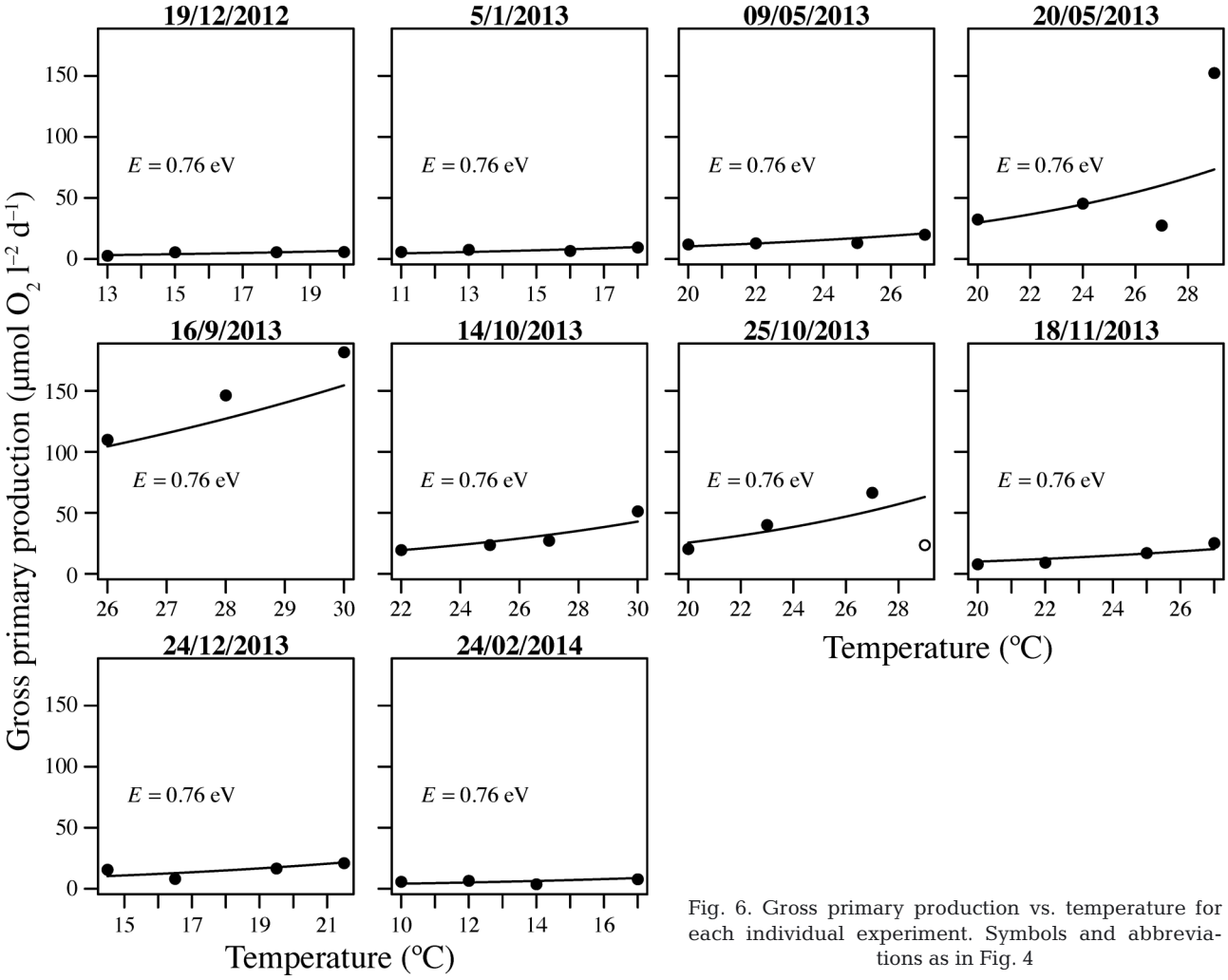

Fig. 6. Gross primary production vs. temperature for each individual experiment. Symbols and abbreviations as in Fig. 4

tions, the random variations associated with the activation energies of growth and grazing rates were usually insignificant, except for the growth rate of picoeukaryotes, a diverse group (Tables 2 & 3).

DISCUSSION

Importance of the abnormally low activation energy of phytoplankton growth and photosynthesis

The Arrhenius equation describing the temperature dependence of metabolism is one core component of the metabolic theory of ecology, although the underlying mechanism is not yet fully understood (Gillooly et al. 2001, Brown et al. 2004). In the foundation paper of the metabolic theory of ecology (Brown et al. 2004), the activation energy was estimated as ~0.65 eV for the metabolism of all organisms including plants. However, since Allen et al. (2005) first proposed that the activation energy of photosynthesis could be as low as 0.32 eV, many studies have confirmed that activation energy differs between autotrophic (photosynthesis or growth) and heterotrophic rates (respiration or grazing) (López-Urrutia et al. 2006, Rose & Caron 2007, O'Connor et al. 2009, Regaudie-De-Gioux & Duarte 2012; but see Taucher et al. 2012). The implication of the lower activation energy of photosynthesis is often stated, for example, as 'our model predicts that there will be a negative feedback of ocean communities to climate warming because they will capture less CO_2 with a future increase in ocean temperature. This feedback of marine biota will further aggravate the anthropogenic effects on global warming' (López-Urrutia et al. 2006, p. 8739). One further implication is that, as the ocean system has to maintain a carbon balance, the ocean needs more carbon subsidy from adjacent areas when temperature rises (Regaudie-De-Gioux & Duarte 2012, Yvon-Durocher et al. 2012).

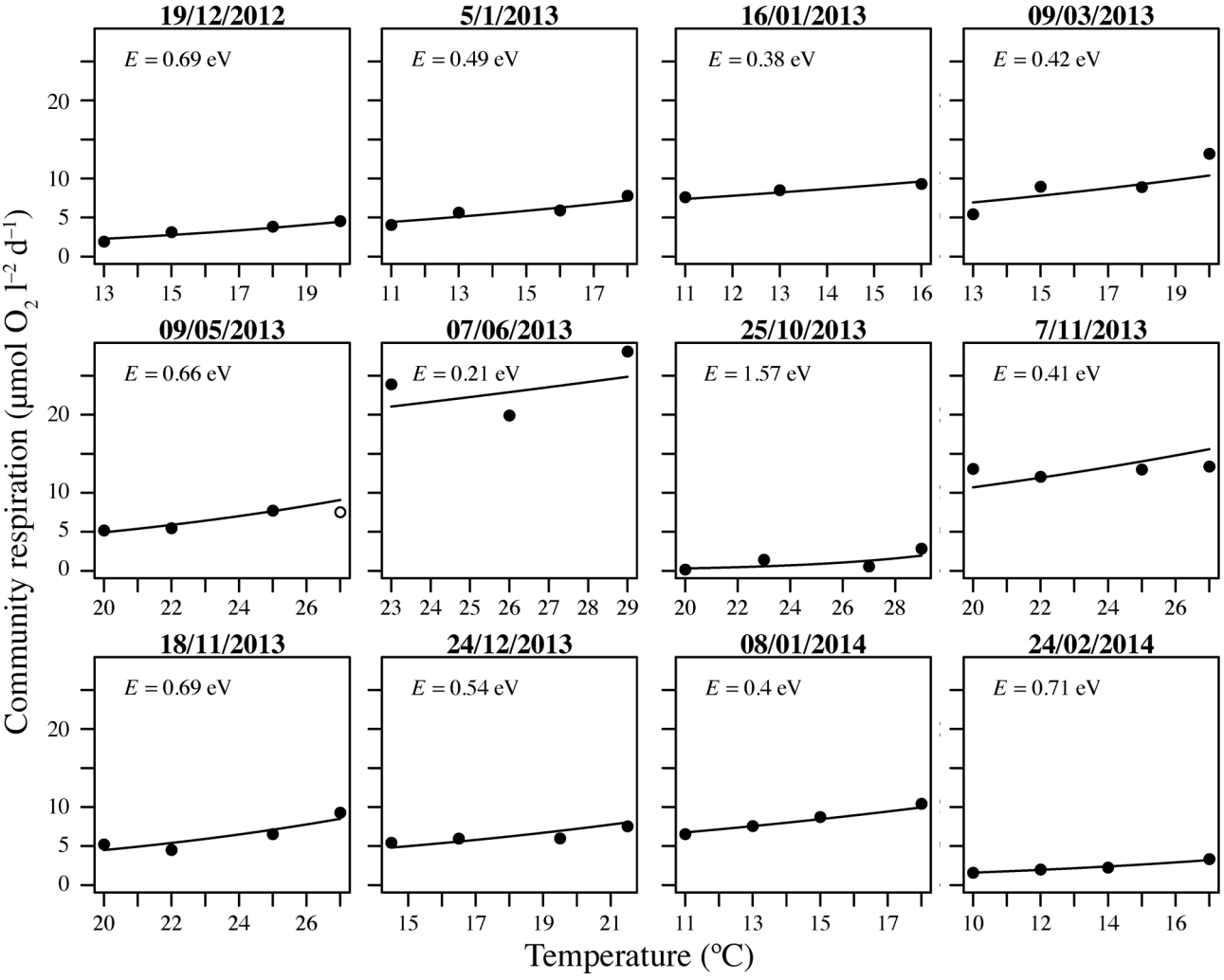

Fig. 7. Community respiration vs. temperature for each individual experiment. Symbols and abbreviations as in Fig. 4

Independent from the development of the metabolic theory of ecology, Laws et al. (2000) also found that the relatively low temperature sensitivity of phytoplankton growth rate can lead to the pattern that high temperature causes low efficiency of carbon export in global oceans, even with the same primary production. The reason is that in warm environments, the processes of nutrient recycling and organic matter decomposition, which are controlled by heterotrophic microbes such as bacteria and protists, are relatively faster than in cold waters so that the particulate organic matter has a lower probability of sinking out of the euphotic zone before being transformed into the soluble phase.

The key problem here is that the activation energy of the photosynthesis or growth rate of autotrophs is 'abnormally' low compared to the 0.65 eV originally proposed by the metabolic theory of ecology (Brown et al. 2004). Such an important problem should be carefully examined.

The physiological basis for the low activation energy of photosynthesis is not well founded

To our knowledge, only Allen et al. (2005) have tried to explain why photosynthesis has a lower activation energy. Based on the thermal kinetics of RuBisCO carboxylation of one transgenic C3 tobacco, Allen et al. (2005) proposed that the key factor leading to the lower activation energy of photosynthesis is the enhanced photorespiration effect at high temperatures. While elegant, this hypothesis is not well suited for marine phytoplankton because most phytoplankton species possess the carbon concentrating mechanisms that allow them to overcome

most effects of photorespiration (Davison 1991, Yvon-Durocher et al. 2010).

If any mechanism that accounts for the low activation energy of photosynthesis is based on the thermal kinetics of enzymatic reactions at subcellular levels, then the activation energy of photosynthesis or phytoplankton growth in response to short-term temperature shifts (as in this study) should be close to 0.32 eV, other things being equal. This is in contrast with our estimates of activation energies of phytoplankton growth and photosynthesis rate in this study (Table 1), suggesting that carbon concentrating mechanisms or other relevant mechanisms might indeed enable the phytoplankton assemblages at our sampling site to overcome the photorespiration effect, although this hypothesis needs to be further tested.

The underlying mechanism controlling the temperature dependence of phytoplankton growth rate is more complicated than of photosynthesis. Although it might be reasonable to assume that under nutrient and light replete conditions, phytoplankton growth rate is limited by photosynthesis, the activation energy of growth rate might differ from that of photosynthesis due to changes of carbon-to-chlorophyll ratios with temperature. And even this assumption may not hold (Stitt & Schulze 1994). Some other processes such as nutrient uptake and assimilation might possibly limit the maximal growth rate of phytoplankton under nutrient and light replete conditions (Marañón et al. 2013). Although there was no significant difference of the activation energy between photosynthesis and growth rate in our study (Table 1), we cannot rule out the possibility that the underlying mechanisms controlling the temperature dependence of phytoplankton growth and photosynthesis can differ.

Potential problems that confound the estimates of activation energy

It is worthwhile to address some potential problems that can affect the estimates of activation energies in this study. The first is that we deliberately removed the data at supraoptimal temperatures at which the simple Arrhenius equation cannot hold. If including all the data in the linear mixed-effect modeling, the activation energies would be 0.55 ± 0.08 and 0.50 ± 0.10 eV, respectively, for phytoplankton growth and photosynthesis rates. Although lower, these estimates are still insignificantly different from 0.65 eV. Previous studies tended not to take into account the pattern of high-temperature inhibition (López-Urrutia et al. 2006, Yvon-Durocher et al. 2010, Regaudie-De-Gioux & Duarte 2012), which we speculate could partially contribute to the low estimates of activation energy of photosynthesis in previous studies.

The second problem is that the temperature extremes in our experimental gradients might impose a 'thermal shock' to the plankton. To minimize this problem, we carefully designed the temperature gradient to ensure that the temperature extremes were not too far away from the *in situ* temperature (see 'Materials and methods'). Although the thermal shock effect cannot be eliminated completely, our estimates of activation energy for grazing and respiration rates are generally within the normal ranges of literature reports (Dell et al. 2011, Fussmann et al. 2014), suggesting that the problem of thermal shock was not severe. The third problem is that the design of abrupt changes of temperature in our experiments cannot address the effect of temperature at evolutionary time scales. As ocean warming occurs at a much slower rate than the experimental warming, the estimates of activation energy obtained from this and other similar studies should be used only cautiously for projecting how marine plankton systems respond to warming.

Temperature sensitivity as a functional trait of plankton

Temperature sensitivity in terms of activation energy is an important parameter in plankton ecosystem models. Although often treated as a constant in models, the activation energies can vary significantly with species and environment, confirmed by the significant random effects in the mixed-effect models (Dell et al. 2011, Huey & Kingsolver 2011, Fussmann et al. 2014). Together with other thermal traits such as optimal temperature (Thomas et al. 2012), these overlooked parameters likely play important roles in affecting the response of plankton dynamics and ecosystem properties to warming. Therefore, it may be necessary to collect more data on the thermal traits of different plankton groups at different locations and times to gain a more accurate understanding of how temperature affects plankton. Previous data compilations are mostly based on the laboratory dataset, while field experiments directly determining the thermal traits of plankton are scarce (Vaquer-Sunyer & Duarte 2013). This study may serve as one of the preliminary studies to provide data on the thermal traits of plankton in the field.

Acknowledgements. We sincerely thank W. Lin, N. Wang, and W. Shen for help in sampling and experimental setups. We also thank 2 anonymous reviewers for their constructive comments on an earlier draft of the manuscript. This study was supported by National Basic Research Program ("973" Program) of China (2015CB954003), National Science Foundation of China (41376130) and Program for New Century Excellent Talents of Xiamen University.

LITERATURE CITED

Allen AP, Gillooly JF, Brown JH (2005) Linking the global carbon cycle to individual metabolism. Funct Ecol 19: 202–213

Bates D, Maechler M, Bolker B, Walker S (2014) _lme4: Linear mixed-effects models using Eigen and S4. R package version 1.1-7, http://CRAN.R-project.org/package=lme4

Bissinger JE, Montagnes DJS, Shaples J, Atkinson D (2008) Predicting marine phytoplankton maximum growth rates from temperature: improving on the Eppley curve using quantile regression. Limnol Oceanogr 53:487–493

Brown JH, Gillooly JF, Allen AP, Savage VM, West GB (2004) Toward a metabolic theory of ecology. Ecology 85: 1771–1789

Chen B, Landry MR, Huang B, Liu H (2012) Does warming enhance the effect of microzooplankton grazing on marine phytoplankton in the ocean? Limnol Oceanogr 57: 519–526

Clarke A (2004) Is there a universal temperature dependence of metabolism? Funct Ecol 18:252–256

Clarke A, Johnston NM (1999) Scaling of metabolic rate with body mass and temperature in teleost fish. J Anim Ecol 68:893–905

Davison IR (1991) Environmental effects on algal photosynthesis: temperature. J Phycol 27:2–8

Dell AI, Pawar S, Savage VM (2011) From the cover: systematic variation in the temperature dependence of physiological and ecological traits. Proc Natl Acad Sci USA 108: 10591–10596

Eppley RW (1972) Temperature and phytoplankton growth in the sea. Fish Bull 70:1063–1085

Faraway JJ (2004) Linear models with R. CRC Press, Boca Raton, FL

Furuya K, Hayashi M, Yabushita Y (1998) HPLC determination of phytoplankton pigments using N,N-dimethylfolmamide. J Oceanogr 54:199–203

Fussmann KE, Schwarzmüller F, Brose U, Jousset A, Rall BC (2014) Ecological stability in response to warming. Nat Clim Change 4:206–210

Gaston KJ, Chown SL, Calosi P, Bernardo J, and others (2009) Macrophysiology: a conceptual reunification. Am Nat 174:595–612

Gillooly JF, Brown JH, West GB, Savage VM, Charnov EL (2001) Effect of size and temperature on metabolic rate. Science 293:2248–2251

Huey RB, Kingsolver JG (2011) Variation in universal temperature dependence of biological rates. Proc Natl Acad Sci USA 108:10377–10378

Landry MR, Haas LW, Fagerness VL (1984) Dynamics of microbial plankton communities: experiments in Kaneohe Bay, Hawaii. Mar Ecol Prog Ser 16:127–133

Landry MR, Brown SL, Rii YM, Selph KE, and others (2008) Depth-stratified phytoplankton dynamics in Cyclone Opal, a subtropical mesoscale eddy. Deep-Sea Res II 55: 1348–1359

Latasa M (2007) Improving estimations of phytoplankton class abundances using CHEMTAX. Mar Ecol Prog Ser 329:13–21

Laws EA, Falkowski PG, Smith JWO, Ducklow H, Mccarthy JJ (2000) Temperature affects export production in the open ocean. Global Biogeochem Cycles 14:1231–1246

Li WKW, Dickie PM (2001) Monitoring phytoplankton, bacterioplankton, and virioplankton in a coastal inlet (Bedford Basin) by flow cytometry. Cytometry 44:236–246

López-Urrutia A, San Martin E, Harris RP, Irigoien X (2006) Scaling the metabolic balance of the oceans. Proc Natl Acad Sci USA 103:8739–8744

Mackey MD, Mackey DJ, Higgins HW, Wright SW (1996) CHEMTAX — a program for estimating class abundances from chemical markers: application to HPLC measurements of phytoplankton. Mar Ecol Prog Ser 144: 265–283

Marañón E, Cermeño P, López-Sandoval DC, Rodríguez-Ramos T and others (2013) Unimodal size scaling of phytoplankton growth and the size dependence of nutrient uptake and use. Ecol Lett 16:371–379

Menden-Deuer S, Lessard EJ (2000) Carbon to volume relationships for dinoflagellates, diatoms, and other protist plankton. Limnol Oceanogr 45:569–579

O'Connor MI, Piehler MF, Leech DM, Anton A, Bruno JF (2009) Warming and resource availability shift food web structure and metabolism. PLoS Biol 7:e1000178

Olson RJ, Zettler ER, Durand MD (1993) Phytoplankton analysis using flow cytometry In: Kemp P, Sherr BF, Sherr EB, Cole JJ (eds) Handbook of methods in aquatic microbial ecology. Lewis Publishers, Boca Raton, FL, p 175–186

Oudot C, Gerard R, Morin P, Gningue I (1988) Precise shipboard determination of dissolved oxygen (Winkler procedure) for productivity studies with a commercial system. Limnol Oceanogr 33:146–150

Parsons TR, Maita Y, Lalli CM (1984) A manual of chemical and biological methods for seawater analysis. Pergamon, Oxford

Putt M, Stoecker DK (1989) An experimentally determined carbon : volume ratio for marine 'oligotrichous' ciliates from estuarine and coastal waters. Limnol Oceanogr 34: 1097–1103

R Core Team (2014) R: a language and environment for statistical computing. R Foundation for Statistical Computing, Vienna

Regaudie-De-Gioux A, Duarte CM (2012) Temperature dependence of planktonic metabolism in the ocean. Global Biogeochem Cycles 26:GB1015, doi:10.1029/2010GB003907

Rose JM, Caron DA (2007) Does low temperature constrain the growth rates of heterotrophic protists? Evidence and implications for algal blooms in cold waters. Limnol Oceanogr 52:886–895

Sal S, López-Urrutia A (2011) Temperature, nutrients, and the size-scaling of phytoplankton growth in the sea. Limnol Oceanogr 56:1952–1955

Sarmiento JL, Slater R, Barber RT, Bopp L and others (2004) Response of ocean ecosystems to climate warming. Global Biogeochem Cycles 18:GB3003, doi:10.1029/2003GB002134

Stitt M, Schulze D (1994) Does Rubisco control the rate of photosynthesis and plant growth? An exercise in molec-

ular ecophysiology. Plant Cell Environ 17:465–487
Strom SL, Fredrickson KA (2008) Intense stratification leads to phytoplankton nutrient limitation and reduced microzooplankton grazing in the southeastern Bering Sea. Deep-Sea Res II 55:1761–1774
Tang EPY (1995) The allometry of algal growth-rates. J Plankton Res 17:1325–1335
Taucher J, Oschlies A (2011) Can we predict the direction of marine primary production change under global warming? Geophys Res Lett 38:L02603, doi:10.1029/2010GL045934
Taucher J, Schulz KG, Dittmar T, Sommer U, Oschlies A, Riebesell U (2012) Enhanced carbon overconsumption in response to increasing temperatures during a mesocosm experiment. Biogeosciences 9:3531–3545
Thomas MK, Kremer CT, Klausmeier CA, Litchman E (2012) A global pattern of thermal adaptation in marine phytoplankton. Science 338:1085–1088
Uye S (1996) Induction of reproductive failure in the planktonic copepod *Calanus pacificus* by diatoms. Mar Ecol Prog Ser 133:89–97
Vaquer-Sunyer R, Duarte CM (2013) Experimental evaluation of the response of coastal mediterranean planktonic and benthic metabolism to warming. Estuar Coast 36: 697–707
Vasseur DA, McCann KS (2005) A mechanistic approach for modeling temperature-dependent consumer-resource dynamics. Am Nat 166:184–198
Vaulot D, Courties C, Partensky F (1989) A simple method to preserve oceanic phytoplankton for flow cytometric analyses. Cytometry 10:629–635
Welschmeyer NA (1994) Fluorometric analysis of chlorophyll *a* in the presence of chlorophyll *b* and pheopigments. Limnol Oceanogr 39:1985–1992
Worden AZ, Binder BJ (2003) Application of dilution experiments for measuring growth and mortality rates among *Prochlorococcus* and *Synechococcus* populations in oligotrophic environments. Aquat Microb Ecol 30:159–174
Yvon-Durocher G, Allen AP, Montoya JM, Trimmer M, Woodward G (2010) The temperature dependence of the carbon cycle in aquatic ecosystems. In: Woodward G (ed) Advances in ecological research. Academic Press, Amsterdam, p 267–313
Yvon-Durocher G, Caffrey JM, Cescatti A, Dossena M, and others (2012) Reconciling the temperature dependence of respiration across timescales and ecosystem types. Nature 487:472–476
Zuur AF, Ieno EN, Walker N, Saveliev AA, Smith GM (2009) Mixed effects models and extensions in ecology with R. Springer, New York, NY

Editorial responsibility: Graham Savidge, Portaferry, UK

Submitted: October 14, 2014; Accepted: January 25, 2015
Proofs received from author(s): April 22, 2015